

Title	Spin polarized transports through a narrow-gap semiconductor wire with ferromagnetic contacts formed on InAlAs step-graded buffer layers
Author(s)	Akabori, M; Yamada, S
Citation	Science and Technology of Advanced Materials, 5(3): 305-308
Issue Date	2004-05
Type	Journal Article
Text version	author
URL	http://hdl.handle.net/10119/3324
Rights	Elsevier, Ltd., Masashi Akabori and Syoji Yamada, Science and Technology of Advanced Materials, 5(3), 2004, 305-308. http://www.sciencedirect.com/science/journal/14686996
Description	

**Spin polarized transports through a narrow-gap semiconductor wire with
ferromagnetic contacts formed on InAlAs step-graded buffer layers**

Masashi Akabori* and Syoji Yamada

Center for Nano Materials and Technology (CNMT), Japan Advanced Institute of
Science and Technology (JAIST), 1-1 Asahidai, Tatsunokuchi, Ishikawa 923-1292,
Japan

*Corresponding author. Tel.: +81-761-51-1477; fax: +81-761-51-1149

E-mail: akabori@jaist.ac.jp (M. Akabori).

Abstract

We investigated the transport properties of ferromagnetic/semiconductor hybrid structures utilizing an InAs/In_{0.75}Al_{0.25}As modulation-doped heterostructures formed on a GaAs (001) substrate with In_xAl_{1-x}As step-graded buffer layers. We used NiFe as ferromagnetic electrodes for injection/detection of spin-polarized electrons, which were formed on side walls of the semiconductor mesa to contact electron channel directly. We measured magneto-transport properties of the samples with current flow between the ferromagnetic electrodes at low temperatures. Under vertical magnetic fields, magneto-resistance oscillations were clearly observed, thus the ferromagnetic electrodes worked as ohmic contacts. In addition, we successfully found spin-valve properties under parallel magnetic fields. Furthermore, we observed the enhancement of spin-valve properties by squeezing the channel width.

Keywords: InAs; InAlAs; 2DEG; Step-graded buffer; Ferromagnetic electrodes; Spin polarized transports

1. Introduction

Recently, semiconductor-based spin devices have been paid much attention because these can control the number of electrons as well as electron spin nature. In particular, spin field effect transistors (spin-FETs) proposed by Datta and Das [1] are one of the most important device, because their operation is based on the combination of spin filter by ferromagnetic (FM) electrodes and spin precession by spin-orbit (SO) interaction of channel electrons. Thus, the spin-FETs consist of non-magnetic semiconductor heterostructures and FM materials.

In order to realize such spin-FETs, we have studied spin transports in non-magnetic $\text{In}_{0.75}\text{Ga}_{0.25}\text{As}/\text{In}_{0.75}\text{Al}_{0.25}\text{As}$ heterostructures having $\text{In}_x\text{Al}_{1-x}\text{As}$ step-graded buffer (SGB) layers on GaAs (001) substrates. We successfully reported control of spin precession by a gate electrode [2] and spin injection from an FM electrode [3]. However, it was difficult to obtain clear spin-valve signals indicating spin injection/detection probably because of the poor contact between the FM electrodes and semiconductors, and the local Hall effects from the FM electrodes.

In this paper, we investigate magneto-transport properties of FM/2DEG hybrid structures with a new narrow-gap heterostructure having a strained InAs two-dimensional electron gas (2DEG) formed on $\text{In}_x\text{Al}_{1-x}\text{As}$ SGB layers. The strained InAs 2DEG is expected to reduce contact resistance of the FM/2DEG interfaces due to

its narrower band gap, and also expected to suppress the local Hall effects due to higher electron concentration of 2DEG. Furthermore, we fabricate both wide-mesa and wire-like channel samples in order to investigate the effects of channel geometry for spin polarized transports.

2. Sample Fabrication

The new heterostructure has 10-nm-thick InAs 2DEG layer on $\text{In}_x\text{Al}_{1-x}\text{As}$ SGB layers as shown in Fig.1a. It was grown by a conventional solid-source molecular beam epitaxy (RIBER 32P). Its electron concentration and mobility at 77 K are $N_S = 7.5 \times 10^{11} \text{ cm}^{-2}$ and $\mu = 4.2 \times 10^4 \text{ cm}^2/\text{Vs}$, respectively. Figure 1b and 1c show schematic and top view of a fabricated hybrid structure. We fabricated two samples with different channel width, $W = 5 \text{ }\mu\text{m}$ (wide-mesa channel sample) and $0.6 \text{ }\mu\text{m}$ (wire-like channel sample). The channel length, L , was fixed to $2 \text{ }\mu\text{m}$. We used electron-beam lithography (ELIONIX ELS-3700) and wet etching with H_2SO_4 -base solution for the fabrication. The FM electrodes consisted of $\text{Ni}_{40}\text{Fe}_{60}$ and were fabricated on side walls of the mesa structures by radio-frequency sputtering process (ANELVA L-100S-FH). We note that Ar-ion etching during 2 minutes in the same chamber was carried out before the formation of FM electrodes to remove native oxides on FM/2DEG contact area.

We measured the magneto-resistance by AC lock-in technique in a conventional liquid He cryostat with a super conducting magnet. Typical measurement temperature was 1.6 K.

3. Results and Discussion

3.1. Magneto-transport properties

Figure 2 shows two-terminal magneto-resistance (MR) characteristics of the wire-like channel sample. The direction of applied magnetic field was vertical to the 2DEG plane, and the current flow was between FM electrodes. We successfully observed clear MR oscillations i.e. Shubnikov de-Haas (SdH) oscillations which indicate well ohmic contacts at FM/2DEG interfaces. We note that the wide-mesa channel sample also showed clear SdH oscillations. Furthermore, we carried out fast Fourier transform (FFT) analysis of MR oscillations to estimate the SO interaction parameter, α . Here, we do not show the result, but some clear peaks could be confirmed in FFT spectrum, which indicate a possibility of electron accumulation in the first subband as well as zero-field spin splitting. With assuming $m^* = 0.03 m_e$, we estimated $\alpha = 17 \sim 27 \times 10^{-12}$ eVm. However, in order to identify such FFT peaks, we have to carry out further experiments and analysis, e.g. characterization of gate-controlled samples.

Figure 3a shows spin-valve properties of the wide-mesa channel sample. The direction of applied magnetic field was parallel to the 2DEG plane and perpendicular to the current flow. Peak-like spin-valve curves corresponding to sweep directions were observed, and the modulation amplitude was about 0.1 %. The results indicate possibility of spin-polarized electron injection and detection between FM electrodes through the InAs 2DEG, and the efficiency of spin injection/detection was simply estimated to be about 3 %, which was equal to square root of 0.1 %. On the other hand, we successfully observed larger modulation of spin-valve curves in the wire-like

channel sample as shown in Fig. 3b. The amplitude was close to 0.5 %, thus the efficiency of spin injection/detection was estimated to be about 7 %. The result suggests that higher efficiency of spin injection/detection can be realized by squeezing channel width.

To clarify the detail of spin-valve properties, we compared spin-valve modulation and contact resistance of samples including a reference $\text{In}_{0.75}\text{Ga}_{0.25}\text{As}$ 2DEG sample as summarized in Table 1. We could confirm the reduction of contact resistance due to narrow-gap InAs 2DEG compared with $\text{In}_{0.75}\text{Ga}_{0.25}\text{As}$. However, by the comparison between wide-mesa channel samples, we found small modulation amplitude of the InAs 2DEG in spite of low contact resistance of FM/2DEG interfaces. Such results indicate that the important points to obtain large modulation signals of spin-valve properties are improvements of FM/2DEG interfaces as well as control of spin polarized transports in channels.

3.2. Model of spin polarized transports in channels

In order to explain the experimental results, we propose the model of spin polarized transport in channels with scattering and spin precession effects. If the transport direction is not perpendicular to the polarized direction as shown in Fig. 4a, spin precession should occur and coherent spin detection cannot be obtained at the drain interface. Furthermore, with longer channel length, scattering events in the channel tend to occur, therefore, coherent spin detection is difficult to be realized as shown in Fig. 4b. Oppositely, coherent spin detection at the drain interface can be realized when a spin polarized electron transports perpendicular to the polarized direction as shown

in Fig. 4c, or total precession is equal to zero as shown in Fig. 4d. In addition, we think that such coherent spin detection tends to increase with narrower channel width due to limiting transport direction.

According to the transport model but neglecting scattering events, we simply calculated spin precession motion for various channel geometry by Monte Carlo method. The details of calculation are shown as follows:

1. At the source interface, spin polarization of electrons is uniform similar to FM polarization.
2. Initial position and transport direction at the source interface is determined randomly.
3. Spin polarized direction is changed during electron motion not perpendicular to FM polarization by spin precession.
4. Electrons are reflected elastically at side walls of channel with keeping spin polarized direction.
5. In the present calculation, coherent spin detection means less than 1 % difference of spin polarized direction at the drain interface.

Calculation parameters are channel length, L , channel width, W , and length of 2π -spin precession, P ($= \hbar^2 / 2\pi m^* \alpha$). In addition, we used effective mass, $m^* = 0.03 m_e$, and the number of calculation was 10000 for a parameter combination (L , W , P). Figure 5a and 5b show calculated spin polarization dependence on W for various L with constant $P = 1 \mu\text{m}$, or for various P with constant $L = 2 \mu\text{m}$. We could clearly find that coherent spin detection would be introduced by shorter L as well as narrower W in spite of neglecting scattering events. Furthermore, we also found that coherent spin detection could be obtained with narrower W less than P as shown by broken guide

line in Fig. 5b. Therefore the results indicate that it is important for spin devices to form small channel structures especially with narrow channel width compared with spin precession.

Finally, we compare the experimental results and the calculation results. From SdH oscillation analysis, we could roughly estimate α as mentioned before, therefore we also could obtain $P = 0.6 \sim 1 \text{ } \mu\text{m}$. The present wire-like channel sample had 0.6- μm -width, and the effective channel width was narrower due to depletion layer from side walls. Therefore, because the effective channel width of the wire-like channel should be narrower than spin precession length, we think that the experimental result of spin-valve enhancement in the wire-like channel sample is consistent with the calculation result.

4. Summary

We fabricated a novel FM/2DEG hybrid structures using an InAs/In_{0.75}Al_{0.25}As modulation doped heterostructure to improve FM/2DEG interfaces, and characterized their magneto-transport properties. We successfully obtained low contact resistance of FM/2DEG interfaces, and also found clear SdH oscillations under vertical magnetic field and spin-valve signals under parallel magnetic field. Furthermore, in a wire-like channel sample, we found the enhancement of spin-valve modulation. Additionally, we proposed simple model of spin polarized transports in the present samples. According to the model, we carried out simple calculation by Monte Carlo method, and demonstrated that the enhancement of spin-valve modulation could be introduced by squeezing the channel width to less than a length of 2π -spin precession.

Acknowledgements

The authors thank Dr. Y. Sato and Dr. T. Kita for fruitful discussions, and Dr. S. Gozu for wafer preparation. This work is partially supported by a Grant-in-Aid for Scientific Research in Priority Areas “Semiconductor Nanospintronics” (No.14076213) of The Ministry of Education, Culture, Sports, Science and Technology, Japan and by Mitsubishi, SCAT, and The Nakajima Foundations for Science and Technology.

References

- [1] S. Datta and B. Das, Appl. Phys. Lett. 56, (1990) 665.
- [2] Y. Sato, T. Kita, S. Gozu and S. Yamada, J. Appl. Phys. 89, (2001) 8017.
- [3] Y. Sato, S. Gozu, T. Kita and S. Yamada, Jpn. J. Appl. Phys. 40, (2001) 1093.

Figure captions

Fig. 1. (a) Layer structure of the InAs 2DEG. (b) Schematic view of fabricated samples.

(c) Top view of the wire-like channel sample.

Fig. 2. Magneto-resistance characteristics of the wire-like channel sample under vertical magnetic field.

Fig. 3. Spin-valve properties of: (a) the wide-mesa channel sample, and (b) the wire-like channel sample.

Fig. 4. Simple model of spin polarized transports in channels. No detection due to: (a) spin precession, and (b) scattering. Coherent detection due to: (c) transport direction perpendicular to polarization, and (d) zero precession in total.

Fig. 5. Calculation result of dependence of spin polarized transports on channel width.

(a) For various channel length, L , with constant precession, $P = 1 \text{ } \mu\text{m}$. (b) For various precession, P , with constant channel length $L = 2 \text{ } \mu\text{m}$.

Table1

Comparison of contact resistance of FM/2DEG interfaces and spin-valve modulation amplitude

Sample	2-term. resistance (Ω)	4-term. resistance (Ω)	Contact resistance (Ω)	Spin-valve amplitude (%)
InAs wide-mesa channel	184	38	73	~0.1
InAs wire-like channel	2237	34	1102	~0.5
In _{0.75} Ga _{0.25} As wide-mesa channel	776	5	386	~0.2
In _{0.75} Ga _{0.25} As wire-like channel	2745	744	1001	~0.5

(a)

In _{0.75} Ga _{0.25} As cap	10 nm
In _{0.75} Al _{0.25} As carrier supply layer	40 nm
In _{0.75} Al _{0.25} As spacer	20 nm
Strained InAs channel	10 nm
In _x Al _{1-x} As SGB layer (x: 0.15~0.75)	
GaAs buffer	
S.I. GaAs substrate	

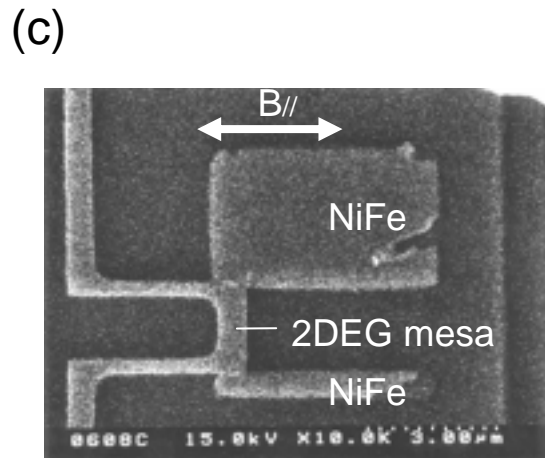
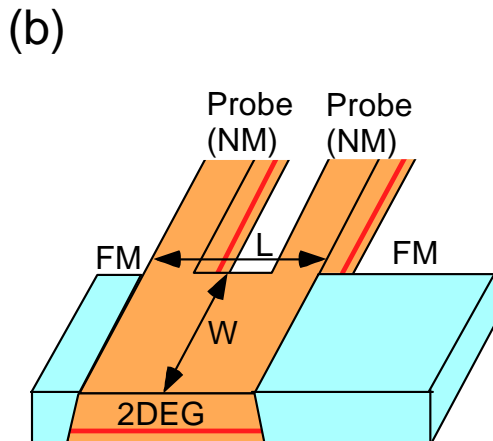


Fig. 1. M. Akabori and S. Yamada

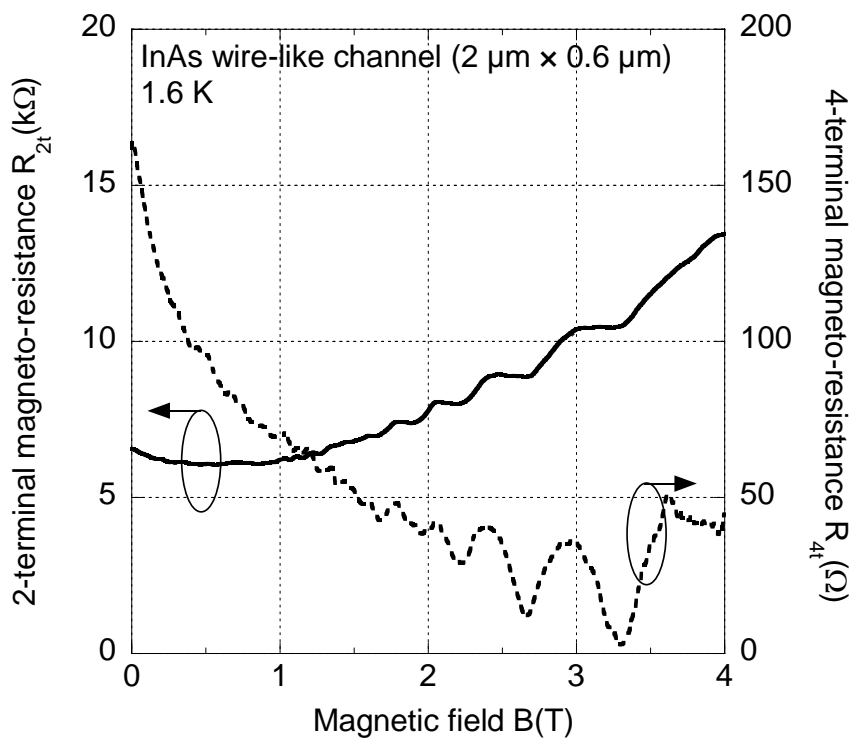


Fig. 2. M. Akabori and S. Yamada

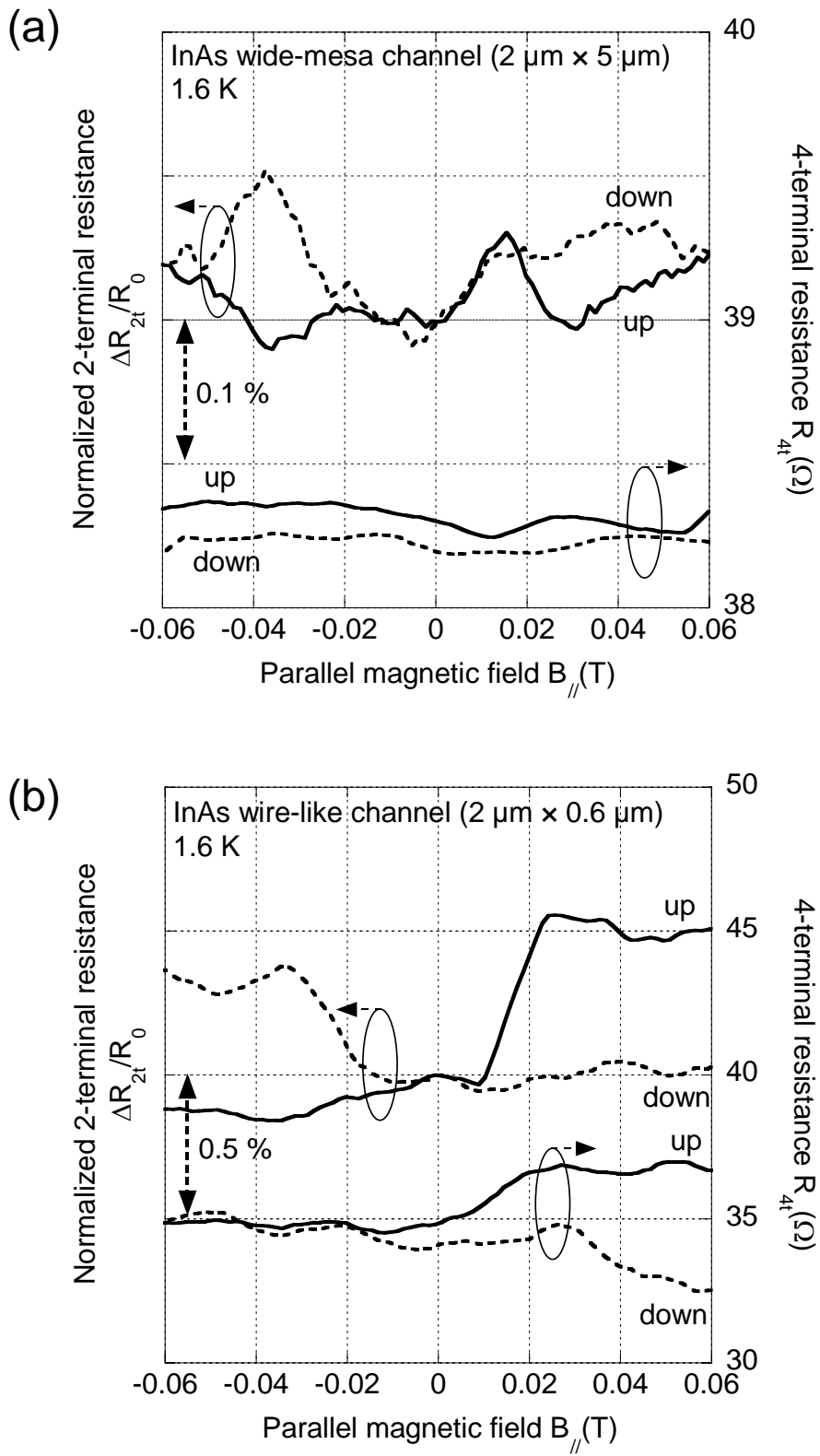


Fig. 3. M. Akabori and S. Yamada

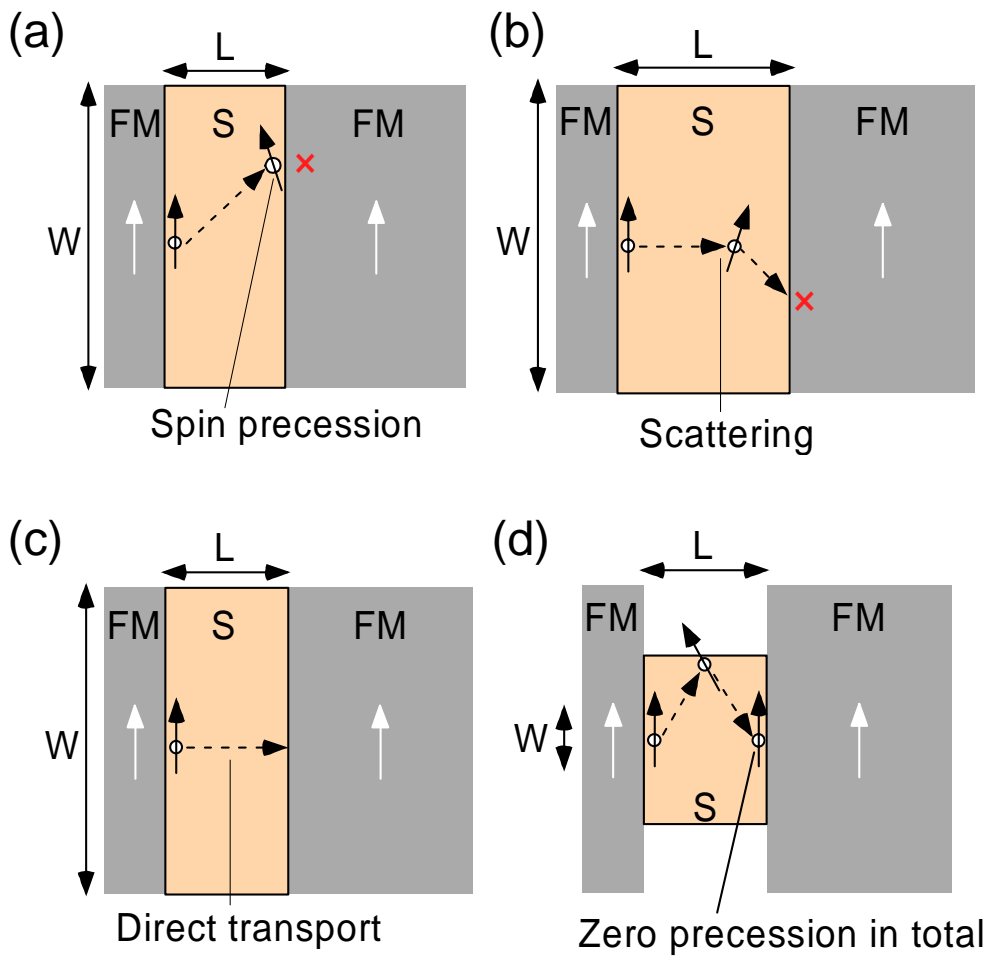


Fig.4. M. Akabori and S. Yamada

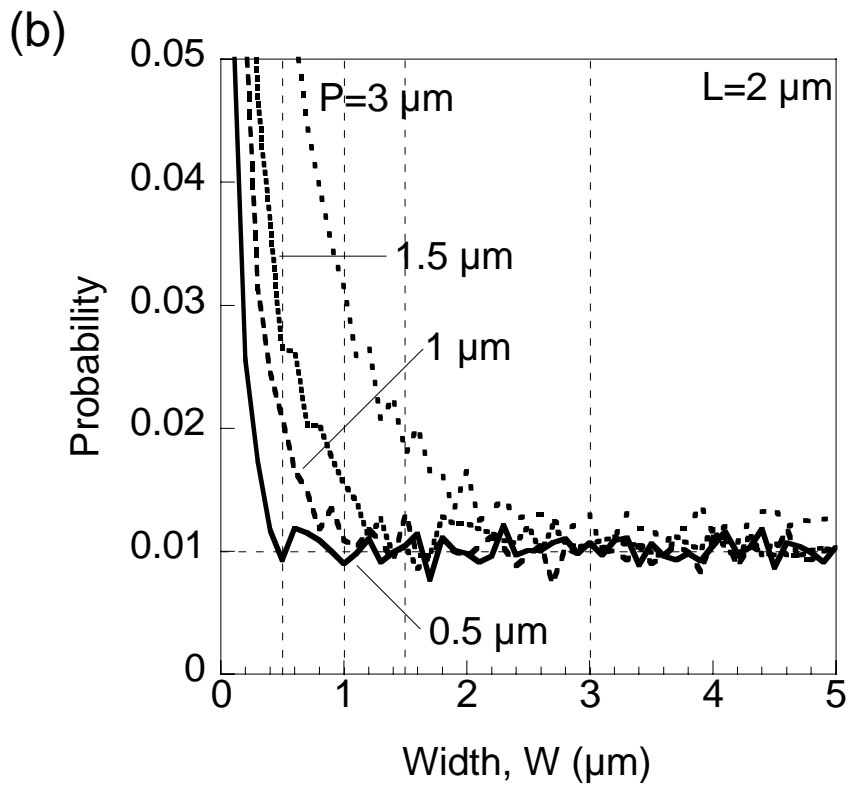
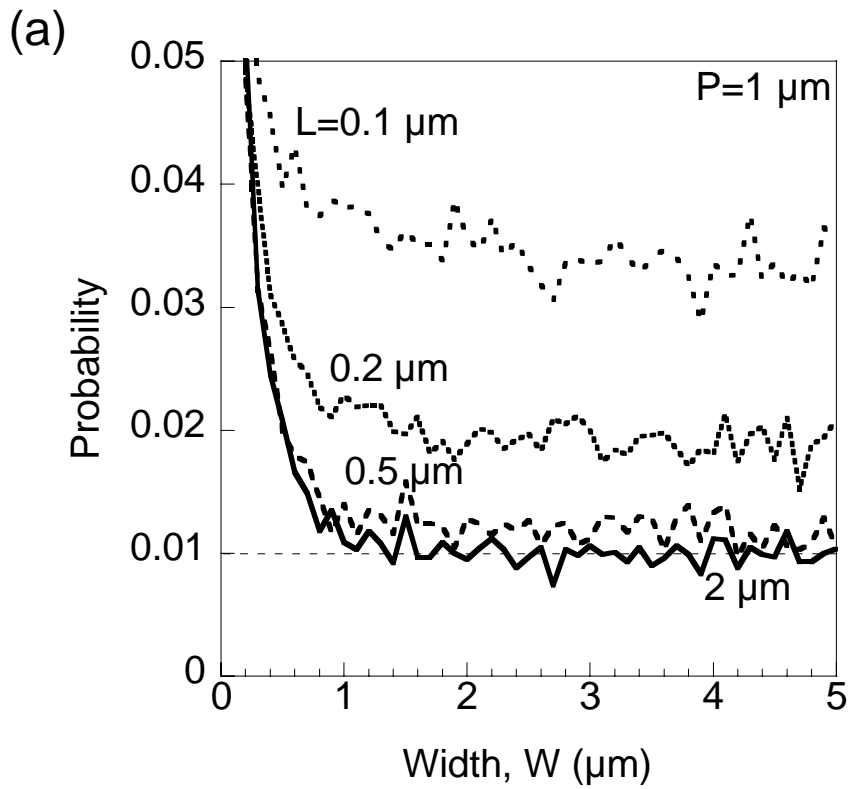


Fig. 5. M. Akabori and S. Yamada